

Full Paper

Sub-Nanoliter Spectroscopic Gas Sensor

Bassam Alfeeli *, Gary Pickrell and Anbo Wang

Center for Photonics Technology, Virginia Polytechnic Institute and State University, 460 Turner Street, Suite 303, Blacksburg, Virginia 24061, USA.

E-mails: alfeeli@vt.edu, pickrell@vt.edu, awang@vt.edu Home page: www.ee.vt.edu/~photonics

* Author to whom correspondence should be addressed.

Received: 31 August 2006 / Accepted: 9 October 2006 / Published: 11 October 2006

Abstract: In this work, a new type of optical fiber based chemical sensor, the sub-nanoliter sample cell (SNSC) based gas sensor, is described and compared to existing sensors designs in the literature. This novel SNSC gas sensor is shown to have the capability of gas detection with a cell volume in the sub-nanoliter range. Experimental results for various configurations of the sensor design are presented which demonstrate the capabilities of the miniature gas sensor.

Keywords: Chemical sensing, Optical sensing, Optical fiber, Miniature gas sensor.

1. Introduction

Medicine, law enforcement, national security, environmental compliance and industrial processes monitoring and control are among the large number of applications that require chemical sensing capabilities. These applications require sensitive, non-destructive, rapid detection and quantification of the chemicals of interest [1]. Most chemical sensing methods are expensive, time consuming, and/or limited in the sampling and analytical techniques which can be applied [2]. Furthermore, only a few laboratory-based sensing techniques have been demonstrated for long-term field measurement applications [3].

Optical sensing techniques have some inherent advantages over other non-optical sensing techniques. Among these advantages are: (a) immunity to electromagnetic interference since the

optical components are highly electrically resistive materials, (b) insensitivity to environmental variations such as temperature and pressure for certain optical sensor designs, and (c) the capability of sensing without having the electronic components located at the measurement environment. Furthermore, the ready availability and continuous development of optical components and instrumentation from the optical communication industry provides an economic advantage to optical sensors. In addition, the use of optical waveguides can provide lower losses over long distances, adding more advantage to the broad area of optical sensing. Optical waveguides can be produced from different materials such as glass, plastic and single crystals. They are relatively inexpensive (except for certain single crystal fibers), robust, flexible, chemically inert, and biocompatible. They also have small physical dimensions, and can be sterilized. Waveguides, such as optical fibers, planer waveguides and hollow-core waveguides, can deliver light to and from the active sensing element over large distances at different locations via multiplexing. This enables real-time, on-line, and multipoint monitoring of large structures and sensing in remote areas that are hazardous, hostile, or difficult to access [4].

Since the invention of optical fibers, research groups have developed various types of optical fiber based sensors [5]. These sensors can be categorized based on light modulation into interferometric and spectroscopic sensors [6]. Fiber Bragg Gratings (FBG's) sensors are the most common types of the interferometric sensors and they make up a significant part of the recent publications on optical fiber sensors [5]. Evanescent Field Absorption (EFA) sensors, which fall under the spectroscopic sensors category, are considered to be the most published type of optical fiber sensor [7]. Hollow-core optical waveguides enabled the development of small sample cell (SC) sensors. Optical fiber based SC sensors are considered to be another type of spectroscopic sensors. All SC sensors reported in [8-13] have cell volumes in the 100's of microliters (μL) range, which is relatively large especially in the age of nanotechnology. However, our research group recently reported a SC sensor for multigas sensing with a cell volume of 3.5 μL [14]. The goal of this work has been to develop and demonstrate a SC gas sensor that has a cell volume in the nanoliter (nL) or sub-nL size range.

Sensor's principle of operation

The use of infra-red (IR) technology in gas sensing is considered one of the most important technologies in industrial, environmental, and safety monitoring [15]. It has been used to provide high-resolution, non-destructive, sensitive, and fast detection and quantification of technologically important chemical species [1]. For the past 15 years, it has been demonstrated, as discussed above, that optical fiber based SC sensors are capable of detecting single and/or multiple gases that have absorption spectra in the near infrared region. This includes O_2 , NO_2 , HF, HBr, H_2O , C_2H_2 , HI, NH_3 , CO, CO_2 , H_2S , CH_4 , and HCl [16]. In general, when the IR radiation passes through a gas cell, a part of the radiation energy will be absorbed by the gas molecules resulting in distinctive absorption bands in the absorption spectrum which allows identification of the chemical species (See figure 1). This spectrum results from the vibrational and rotational energies of the particular species being measured.

Incident light, with a frequency equal to one of the vibrational or rotational energies of the species being considered, can be absorbed by the gas species.

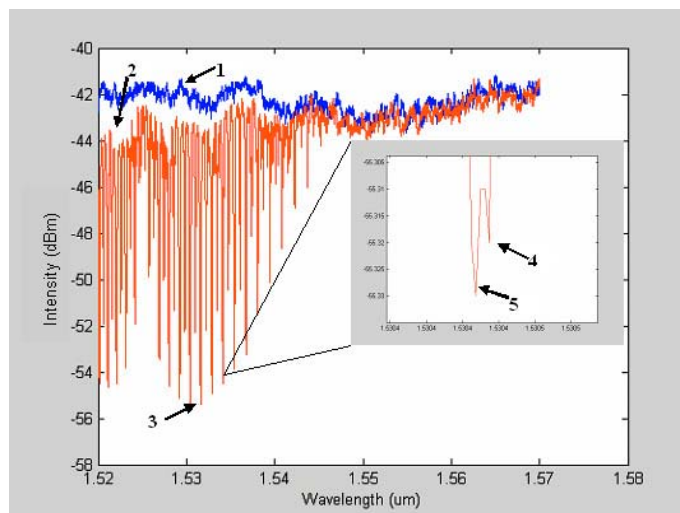


Figure 1. Absorption spectrum of Acetylene as measured by the newly developed SNSC optical fiber based sensor with features common in IR spectra: (1) Baseline (2) Area between baseline and transmitted light line representing background absorption or reflection losses (3) Absorption maximum of the vibration-rotation lines representing the maximum uptake of radiation energy by the acetylene molecules (4) $^{13}\text{C}_2\text{H}_2$ isotope maxima (5) $^{12}\text{C}_2\text{H}_2$ isotope maxima.

As shown in Figure 1, features 4 and 5 represent the separation of the line's maximum into two maxima. This phenomenon is explained by the isotope effect. The shift of maximum line position is due to the fact that the two isotopes have two different masses. The simultaneous presence of acetylene isotopes gives rise to the splitting of the line maximum [17]. This ability to separate out even the isotopes of the same gas chemistry shows the tremendous resolving power in the wavelength domain that is afforded by this SNSC type of optical sensor design.

The SNSC sensor consists of an IR source, a gas cell, and an IR detector. An optical fiber, acting as a transmission medium, delivers the IR radiation to the micro capillary tubing which serves in an analogous fashion to the traditional gas cell. The light passes through the sample contained in the micro capillary tubing to another optical fiber, acting as a receiver, which delivers the altered IR radiation to the detector (See figure 2).

Near-IR spectroscopy is governed by the Beer-Lambert law. In mathematical terms, this relation is expressed as

$$A = \epsilon cl \quad (1)$$

where A is the absorbance of the sample, c is the concentration, l is the path length of the sample, and ϵ is a constant that depends on the absorptivity of the species at a particular wavelength. Absorbance is defined as the logarithmic ratio of the intensity of the incident to detected light. In addition, light attenuation should be considered when fabricating a gas cell out of dielectric hollow-core optical

waveguide. It has been shown by Miyagi and Nishida that the attenuation constant is related to the wavelength of the light and the hollow core radius by

$$\alpha \propto \frac{\lambda^3}{r^4} \quad (2)$$

where α is the attenuation constant, λ is wavelength, and r is the inner radius of the hollow waveguide [18].

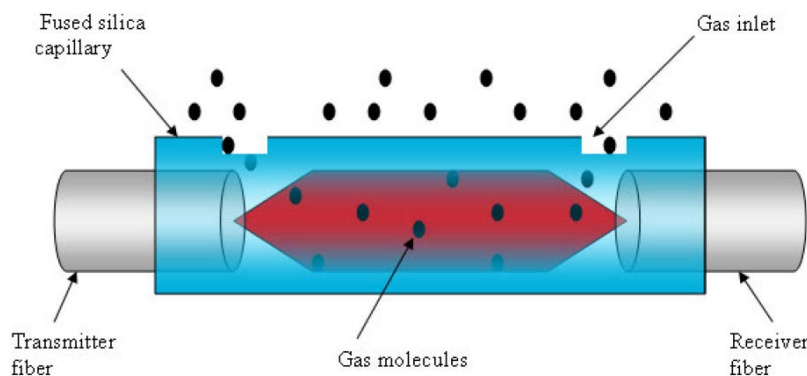


Figure 2. Sample cell gas sensor.

This means that in very small core hollow waveguides there will be more light propagating in the glass wall than in the hollow core. From equations 1 and 2, one can see that there are trade-offs to be considered in the design of the sensor. The price of decreasing the gas cell dimensions is a decrease in absorbance and an increase in light attenuation. Thus, small gas cell design requires good signal processing techniques to improve signal-to-noise (S/N) ratios. Furthermore, limiting the number of gases to be detected, that is, using a narrow-linewidth optical source increases the value of the absorptivity coefficient. Therefore, it is extremely difficult to realize a sensor with a nL volume gas cell without sacrificing the sensitivity of the sensor and limiting the number of gases to be detected simultaneously.

2. Experiment

Sensor fabrication and experimental setup

The dimensional limitation imposed by equations 1 and 2 necessitate the determination of the dimensional lower limits of the gas cell. The geometrical shape of the cell is cylindrical where the area of the base is equivalent to the area of the cross section of the hollow core and the cylinder's height is equivalent to the optical path length. The objective of the experimental setup below is to establish the minimum bore size and optical path length for the nL volume SC sensor. This setup is also intended to determine the sensitivity and response time of the sensor.

Due to the small dimensions of the sensors, the construction of the sensors was done with the aid of an optical microscope. The sensors were fabricated by using hollow fused silica micro capillary tubes

from Polymicro Technologies, LLC, and SMF-28 single-mode fibers from Corning, Inc. Openings on the surface at the middle of the tubes were made for the gas to flow in and out the micro capillary tubings. A mid-range 50 mJ Excimer Laser MSX-250 from MPB Technologies Inc. was used to produce the holes in the capillary tubes. The tubes were then flushed with acetone to wash away any glass debris which resulted from the hole making process. For tubes with bore sizes larger than 125 μm , the transmitter and receiver fibers were inserted in the tube and sealed with epoxy. For tubes with bore size smaller than 125 μm the transmitter and receiver fibers were bonded to the ends of the tube by fusion bonding made by Sumitomo Type-36 Fusion Splicer. All fabricated sensors were inspected visually under the microscope before testing.

The details of the experimental apparatus to control the admission of gases and removal of gases from the sensor regions have been described previously [14]. In fact, the same apparatus was used in this study (See Figure 3). It consists of an assembly of stainless-steel pipes connected through valves to an acetylene gas tank and a vacuum pump. To test the sensor, the sensor was installed in one of the stainless-steel pipes and sealed with epoxy. A component testing system (CTS) from Micron Optics Inc. was used as an optical interrogation system. The high-resolution swept laser system contains a fiber ring laser that is continuously swept from 1520 to 1570 nm and has dynamic range of detection capability of more than 60 dBm. The choice of acetylene as a testing gas was a matter of convenience. Any gas or a mixture of gases that have absorption spectra in 1520 to 1570 nm range would be able to be detected by the sensor. Acetylene has been typically used in testing near infrared sensors [14-16, 19-22].

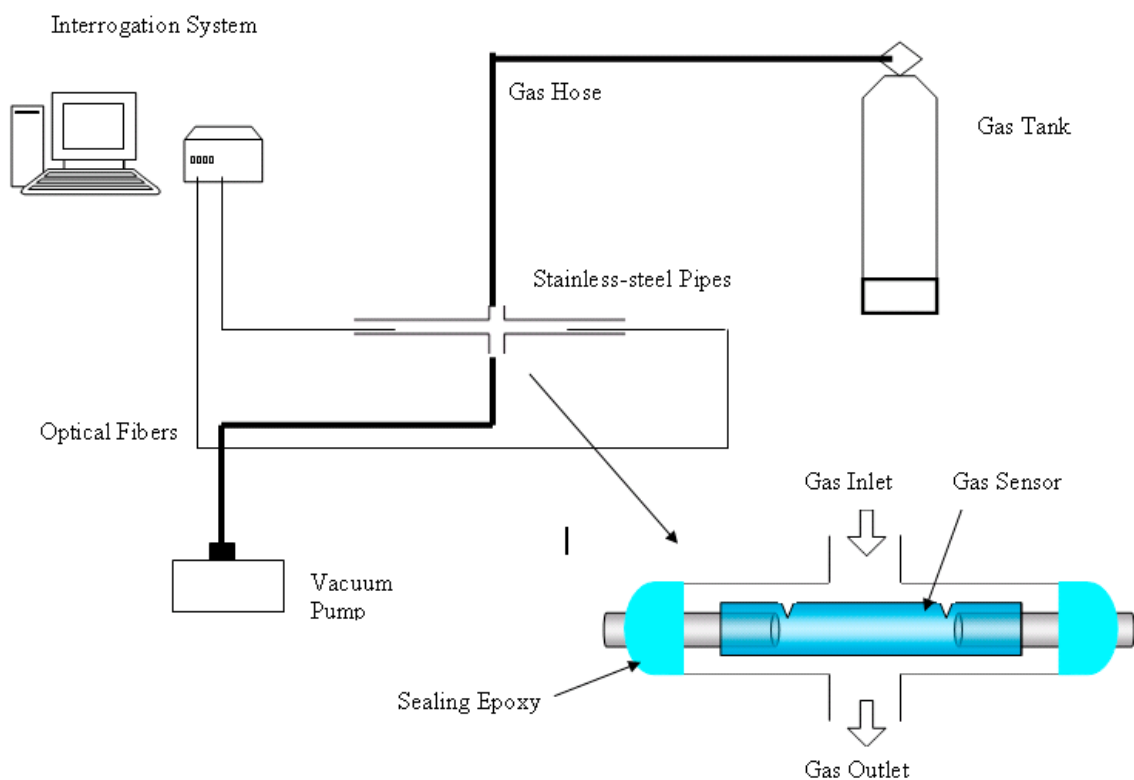


Figure 3. Experimental setup.

Before starting the experiment, the setup was evacuated for 3 minutes using a vacuum pump and then filled with acetylene gas to the desired pressure. The stainless-steel pipes have large enough inner diameter to house several sensors, thus, enabling multiple sensors with different gas cell dimensions to be tested under the same conditions. For the response time study, the measurement was done by purging the gas and collecting spectra data at timed intervals.

3. Results and Discussion

To determine the minimum bore size for the SNSC sensor gas cell, five sensors with the same optical path length of 50 mm and bore size ranging from 2 μm to 134 μm were fabricated and tested under a static pressure of 10 Psi and at room temperature. Table 1 lists the gas cell bore sizes with their corresponding volumes. Because the absorption spectra consist of a series of absorption lines in two sets, the average of odd number absorption lines of the P-branch that are conventionally labeled from P(1) to P(19) were used to report the results shown in figure 4. This was done for consistency purposes. Each data point in the figure 4 represents the average intensity magnitude of the selected 10 absorption lines. The results show a significant drop in the absorption intensity for the 10 μm and 2 μm bore size sensors. The reason for such drop in intensity can be attributed to the fact that more light propagates in the glass wall than in the hollow core. Thus, for reliable detection, the minimum bore size for the gas cell in the SNSC sensor should be around 25 μm .

Table 1. Gas cell bore sizes with their corresponding volumes at fixed path length of 50 mm.

Bore size (μm)	Gas cell volume (nL)
2	0.16
10	3.93
25	24.5
75	221
134	705

To determine the minimum path length for the gas cell of the SNSC sensor, nine sensors with path lengths ranging from 125 μm to 250 mm were fabricated and tested under a static pressure of 20 Psi at room temperature. Table 2 lists the gas cell path lengths with their corresponding volumes. Similar to the bore size study, the odd number lines from P(1) to P(19) were measured in each of the nine sensors spectra and then averaged. The results are shown in figure 5. Each data point in the figure 5 also represents the average intensity magnitude of the selected 10 absorption lines. The absorption intensities were below the detection limits of the optical interrogation system used for the 0.125 mm path length (not shown in figure 5). The 1 mm path length sensor showed an average intensity of about 0.18 dBm whereas the 250 mm path length sensor showed an average intensity of 21.6 dBm. Thus, for reliable detection, the minimum path length for the gas cell in the SC sensor should be around 1 mm.

According to the results presented, a SC sensor with a gas cell volume as small as 0.5 nL can reliably produce absorption lines above the noise level of the system.

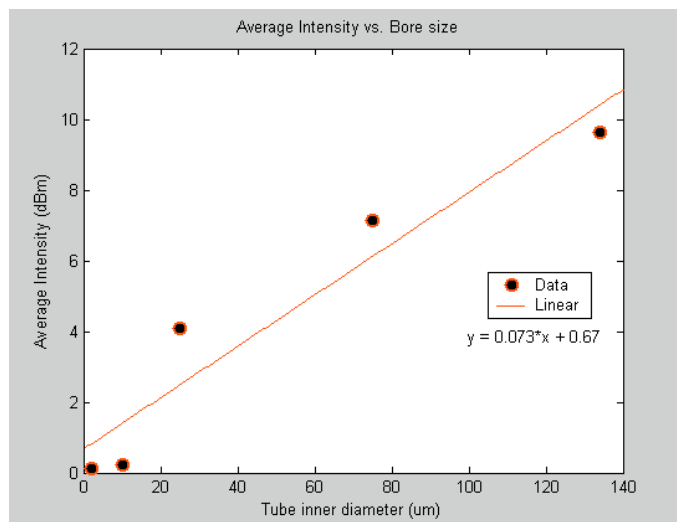


Figure 4. Average Intensity vs. Bore size (50 mm path length) at 10 Psi.

Table 2. Gas cell path lengths with their corresponding volumes at fixed bore size of 134 μm.

Path length (mm)	Gas cell volume (nL)
0.125	1.76
1	14.1
2	28.2
5	70.5
10	141
15	211
50	705
100	1410
250	3520

To compare the sensitivity of the sub-nL volume sensor to the μL volume sensor, the response of the two sensors to different levels of applied pressure of acetylene was investigated. This was done by fabricating two sensors. One with 3.5 μL volume gas cell and another with 0.5 nL volume gas cell. It should be noted that the two sensors are made of the same material and have similar structures. The major difference between the two is the gas cell volume. As expected from equation 1, the results shown in figure 6 and figure 7 demonstrate that the two sensors response in similar manner but the magnitude of the response is not the same. The objective here is to demonstrate that the sub-nL volume sensor is capable of detecting different concentrations of acetylene. It should be noted that the

sensor was also capable of detecting low concentrations as shown by the data point below zero relative pressure.

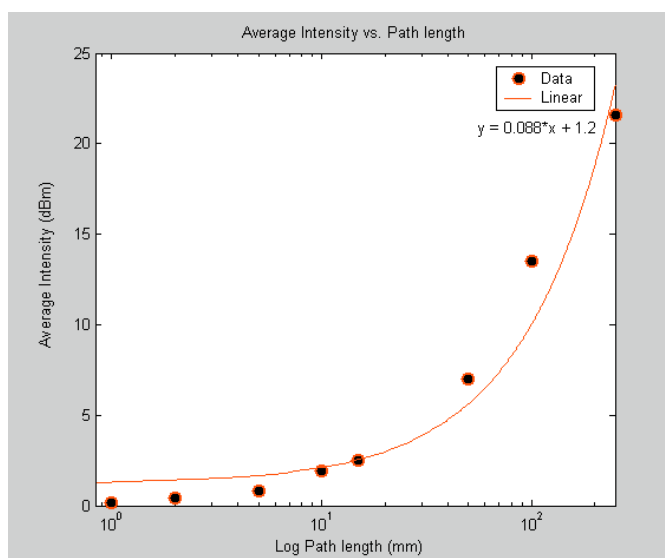


Figure 5. Average Intensity vs. Path length (134 μm bore size) at 20 Psi.

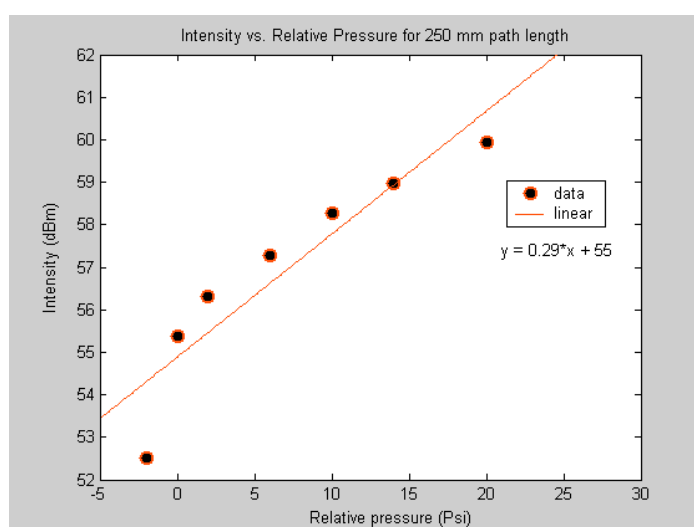


Figure 6. Intensity vs. Pressure for 250mm path length (134 μm bore size).

Moreover, pressure broadening effect was observed when the spectra of different pressure levels were superimposed. Zooming in at any of the absorption lines reveals the pressure broadening effect. The broadening of absorption lines in a spectrum occurs as a result of collisions between excited molecules [23]. Pressure broadening, also known as collision broadening, is demonstrated in figure 8. In this figure, the red, green and blue lines represent spectra at pressure levels: below atmospheric pressure, at atmospheric pressure, and 5 Psi respectively.

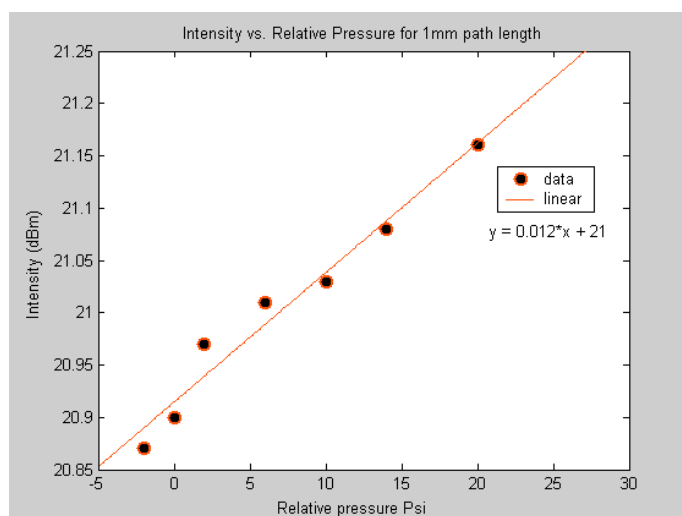


Figure 7. Intensity vs. Pressure for 1mm path length (25 μm bore size).

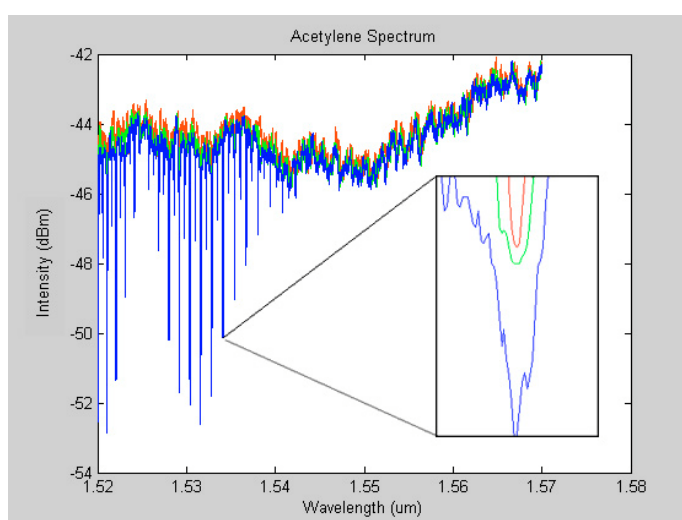


Figure 8. Pressure broadening

If we ignore all other broadening mechanisms, the absorption lines have natural width. The line width of an absorption line in a spectrum is governed by the Heisenberg uncertainty principle.

$$\text{Linewidth}_{\text{natural}} = \frac{1}{2\pi c\Delta t} \quad (3)$$

where c is the speed of light and Δt is the lifetime of the excited state. However, natural broadening is not considered in the determination of the width of the lines. Only, Doppler, collision broadening or their combination is considered in line width calculations. The Doppler Effect occurs due to the direction of motion of individual molecules with respect to the light passing through it. Doppler broadening varies with temperature and molecular weight but it is independent of pressure. On the

other hand, collision broadening is linearly proportional to the pressure. Collision broadening determines the profile of the absorption line when the gas present is at certain pressure level. The half-width pressure broadening is given by

$$\text{Linewidth}_{\text{collision}} = \text{Linewidth}_{\text{atmosphere}} p \quad (4)$$

where p is the pressure and $\text{Linewidth}_{\text{atmosphere}}$ is the half-width at 1 atmospheric pressure [24]. The pressure broadening effect observed in figure 8 could be valuable since it gives information about the pressure of the detected gas.

To compare the response time of the SNSC sensor to the μL volume sensor, the time required for the acetylene gas to diffuse out of the gas cell for the two sensors was measured. The decay curves shown in figures 9 and 10 correspond to the response time of the μL and sub-nL sensors respectively. The response time measurement is limited by the time required to open the gas valve and acquire the transmission signal. It takes at least 10 seconds for the operator to open the valve and start taking snapshots of the spectrum. It appears as the sensor has almost instantaneous response to change in concentration. The absorption line intensity drops sharply as soon as the gas starts to flow out of the gas cell. Since the gas is under pressure, the flow rate decays exponentially with time as the pressure in the gas cell gets equalized.

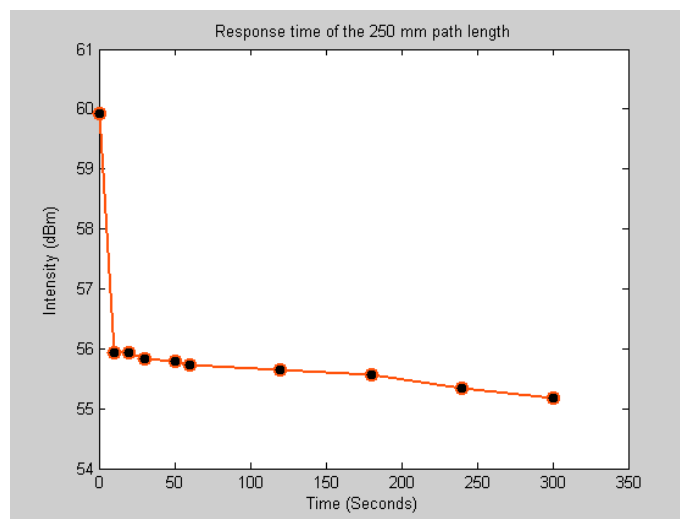


Figure 9. 250mm Path Length (134 μm bore size) Response time.

The minimum detectable concentration can be derived by manipulating equation 1 and is written as

$$C_{\min} = \frac{\left(\frac{I_o - I}{I_o} \right)_{\min}}{(\varepsilon l)_{\max}} \quad (5)$$

where C_{\min} is the minimum detectable concentration, I_o is the incident light intensity, I is the detected light intensity, l is the optical path length, and ε is a constant that depends on the absorptivity of the species at a particular wavelength. Equation 5 reveals that the detection limit is determined by the path

length and the S/N ratio in the spectrum. Since only lines above the noise level in a spectrum can be detected, the reduction of noise can directly correspond to an increase in the detectability. The noise level is a function of the detector, number of scans, spectral resolution and source intensity. The interrogation system used in this work has an extremely low-noise laser source and can resolve wavelengths down to 0.25 pm. Thus, the system should produce a very low noise level. Additional noise reduction could be accomplished by using longer measurement time. This was done by setting the system to sweep across the spectrum at a rate of 0.5 Hz instead of default 5 Hz scan rate.

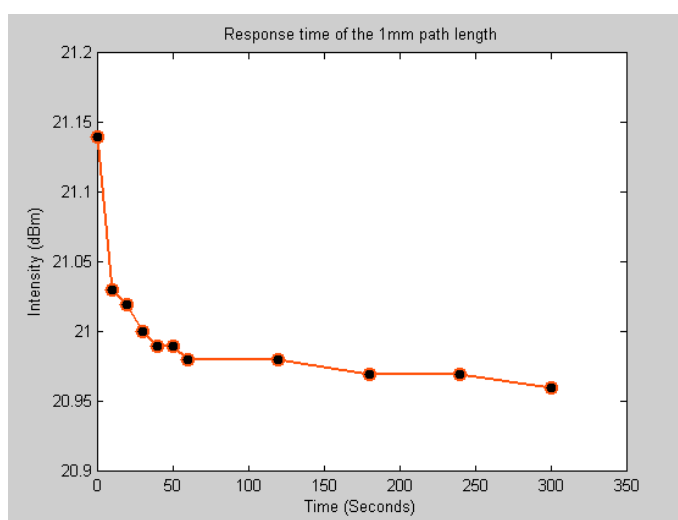


Figure 10. 1mm Path Length (25 μm bore size) Response time.

By using the high-resolution interrogation system a detectable intensity change as small as 0.01 dBm can be observed. For the μL volume sensor (250mm path length) and assuming $\varepsilon = 0.725 \text{ cm}^{-1}$ for acetylene, the minimum detectable concentration is less than 10 ppm. For the SNSC sensor, the minimum detectable concentration is around 1000 ppm. For reference, the standard minimum detection limit as reported in [25] for acetylene in a 100 m path length measured in air is 0.15 ppm.

Conclusions

In this work, an optical fiber SC sensor with gas cell in the sub-nL volume range has been fabricated and tested. The experimental results demonstrated the capabilities of the miniature gas sensor. The sub-nL SC sensor currently has not achieved the same sensitivity as the currently available gas sensors but it offers simple, real-time, inexpensive, robust, flexible, miniature, chemically inert, and biocompatible sensor for applications that does not require high sensitivity. Further research may allow an increase in the sensitivity of this newly demonstrated sensor. The sensor's performance in harsh environments will be also evaluated in future work.

Acknowledgements

This work was financially supported by the Kuwait Institute for Scientific Research (KISR), Kuwait.

References

1. Blake, T.A.; Kelly, J.F.; Stewart, T.L.; Hartman, J.S.; Sharpe, S.W.; Sams, R.L. Absorption spectroscopy in hollow-glass waveguides using infrared diode lasers. *Diode Lasers and Applications in Atmospheric Sensing* **2002**, Proceedings of SPIE, 4817, 216 - 232
2. Ho, C.K.; Robinson, A.; Miller, D.R.; Davis, M.J. Overview of sensors and needs for environmental monitoring. *Sensors* **2005**, 5(1-2), 4-37.
3. Farries, M.C.; Shaw, A.M.; Fisk, J.; Garvey, L. Detection of low chemical concentrations by cavity ring-down in an evanescently coupled fused optical fibre taper. *Optically Based Biological and Chemical Sensing for Defence* **2004**, SPIE, 5617, 334-340
4. Alfeeli, B. Miniature gas sensing device based on near-infrared spectroscopy, *Master of Science Thesis*, Electrical and Computer Engineering, Virginia Polytechnic Institute and State University, Blacksburg, VA, **2005**
5. Webb, D.J. Optical-fiber sensors: an overview. *MRS Bulletin* **2002**, 27(5), 365-9.
6. Culshaw, B. Fiber-optic sensors: applications and advances. *Optics & Photonics News* **2005**, 16(11), 24-9.
7. Lehmann, H.; Brueckner, S.; Kobelke, J.; Schwotzer, G.; Schuster, K.; Willsch, R. Toward photonic crystal fiber based distributed chemosensors. *17th International Conference on Optical Fibre Sensors* **2005**, SPIE, 5855, 419-422
8. Saggese, S.J.; Harrington, J.A.; Sigel, J.G.H. Hollow and dielectric waveguides for infrared spectroscopic applications. *Applied Spectroscopy in Material Science* **1991**, SPIE, 1437, 44-53
9. Saggese, S.J.; Harrington, J.A.; Sigel, G.H., Jr.; Altkorn, R.; Haidle, R. Novel lightpipes for infrared spectroscopy. *Applied Spectroscopy* **1992**, 46(7), 1194-7.
10. Saito, M.; Sato, S.-y.; Miyagi, M. Spectroscopic gas sensing with infrared hollow waveguides. *Chemical, Biochemical, and Environmental Fiber Sensors IV* **1993**, SPIE, 1796, 231-242
11. Kozodoy, R.L.; Micheels, R.H.; Harrington, J.A. Small-Bore Hollow Waveguide Infrared Absorption Cells for Gas Sensing. *Applied Spectroscopy* **1996**, 50(3), 415 - 417.
12. Worrell, C.A.; Gallen, N.A. Trace-level detection of gases and vapours with mid-infra-red hollow waveguides. *J. Phys. D: Appl. Phys.* **1997**, 30, 1984 - 1995.
13. Haan, D.J.; Harrington, J.A. Hollow waveguides for gas sensing and near-IR applications. *The SPIE Conference on Specialty Fiber Optics for Medical Applications* **1999**, SPIE, 3596, 43 - 49
14. Peng, W.; Pickrell, G.R.; Shen, F.; Wang, A. Experimental Investigation of Optical Waveguide-Based Multigas Sensing. *IEEE Photonics Technology Letters* **2004**, 16(10), 2317 - 2319.
15. Stewart, G.; Whitenett, G.; Shields, P.; Marshall, J.; Culshaw, B. Design of fibre laser and sensor systems for gas spectroscopy in the near-IR. *Industrial and Highway Sensors Technology* **2004**, Proceedings of SPIE, 5272, 172 - 180

16. Pickrell, G.; Peng, W.; Wang, A. Random-hole optical fiber evanescent-wave gas sensing. *Optics Letters* **2004**, *29*(13), 1476 - 1478.
17. Houghton, J.T.; Smith, S.D. *Infra-red Physics*. Oxford University Press. **1966**.
18. Miyagi, M.; Nishida, S. Transmission Characteristics of Dielectric Tube Leaky Waveguide. *IEEE Transactions on Microwave Theory and Techniques* **1980**, *MTT-28*(6), 536-541.
19. Cheung, A.; Johnstone, W.; Moodie, D. Detection of acetylene gas using optical correlation spectroscopy. *17th International Conference on Optical Fibre Sensors* **2005**, SPIE, *5855*, 475-478
20. Stewart, G.; Whitenett, G.; Marshall, J.P.; Johnstone, W.; Culshaw, B.; MacLean, A.; Mauchline, I.S.; Moodie, D.G. Remote gas analysis using fibre optic links and near infrared absorption. *Optical Sensing* **2004**, SPIE, *5459*, 285-294
21. Zhang, Y.; Zhang, M.; Jin, W.; Ho, H.L.; Demokan, M.S.; Culshaw, B.; Stewart, G. Investigation of erbium-doped fiber laser intra-cavity absorption sensor for gas detection. *Optics Communications* **2004**, *232*(1-6), 295-301.
22. Ritari, T.; Tuominen, J.; Ludvigsen, H. Gas sensing using air-guiding photonic bandgap. *Optics Express* **2004**, *12*(17), 4080 - 4087.
23. Denney, R.C. *A Dictionary of Spectroscopy*. 2 ed. Wiley & Sons, Inc. New York, **1982**.
24. Wormhoudt, J., ed. *Infrared Methods for Gaseous Measurements: Theory and Practice*. Optical Engineering, ed. B.J. Thompson. Vol. 7, Marcel Dekker, Inc., **1985**.
25. Sigrist, M.W., ed. *Air Monitoring by Spectroscopic Techniques*. Chemical Analysis, ed. J.D. Winefordner. Vol. *127*, **1994** John Wiley & Sons, Inc.